Comparative Study of Rotor PM Transverse Flux Machine and Stator PM Transverse Flux Machine with SMC Cores

Chengcheng Liu[1,2], Xue Wang[1,2], Youhua Wang[1,2], Gang Lei[3], Youguang Guo[3], and Jianguo Zhu[4]

[1] State Key Laboratory of Reliability and Intelligence of Electrical Equipment (School of Electrical Engineering, Hebei University of Technology), Tianjin 300130, China

[2] Province-Ministry Joint Key Laboratory of EFEAR, Tianjin 300130, China

[3]School of Electrical and Data Engineering, University of Technology Sydney, Ultimo, NSW 2007, Australia

[4]School of Electrical and Information Engineering, University of Sydney, Sydney, NSW 2006, Australia

Corresponding author: C. Liu (email:2016020@hebut.edu.cn)

Abstract

With the adoption of 3D magnetic flux material and global ring windings, permanent magnet transverse flux machine (PMTFM) with soft magnetic composite (SMC) cores can output relatively high torque density and only require easy manufacturing process. For the PMTFM, there are two ways to put the permanent magnets (PMs). One is to put the PMs on the rotor side which is the traditional rotor PM TFM and the other is to put the PMs on the stator side which is the stator PM TFM. In this paper, the design methods and operation principle for both kinds of PMTFM will be presented and discussed. Four different TFMs (benchmark rotor PM TFM with NdFeB, stator PM TFM1 with ferrite magnet and stator PM TFM2 and TFM3 with NdFeB) have been designed, and the magnetic parameters and the main performance will be comparatively studied to show the main difference between stator PM TFM and rotor PM TFM. It can be seen that the stator PM TFM has better performance, and the stator PM TFM1 with ferrite magnets can have the same torque ability as that of the rotor PM TFM with NdFeB magnet but with very low material cost. With the adoption of NdFeB, the stator PM TFM2 can have two times higher torque ability than the rotor PM TFM, and the stator PM TFM2 can have the same torque ability as that of rotor PM TFM but with much smaller volume. As for the power factor and efficiency, it can be seen that the adoption of ferrite magnet will reduce both of them, and there is no much difference for the place where the PMs are installed.

Key Words: Soft magnetic composite (SMC), permanent magnet (PM) transverse flux machine, stator PM, rotor PM, NdFeB magnet, ferrite magnet.

Introduction

Soft magnetic composite (SMC) material is one kind of relatively new soft magnetic material, and it owns many unique properties, e.g. thermal and magnetic isotropy characteristic and very low eddy current losses, compared with the traditional silicon steels, but it also has the disadvantages of low permeability and weak mechanical performance[1-3]. With appropriate machine topology and design guidelines, electrical machines with SMC cores can have better performance than the traditional electrical machines[4-6]. For the better utilization of SMC in electrical machine, some key design guidelines should be followed. Firstly, SMC machine should be designed with permanent magnet (PM) excitation. Secondly, it should be designed with higher frequency operation, and thirdly, it should be designed with 3-D magnetic flux path. Currently, many powder metallurgy companies are investing greatly for the magnetic and mechanical performance improvement of the SMC cores for electrical application, and some electrical machines with SMC cores have appeared for some small scale applications[7].

In the past decades, various kinds of electrical machines with SMC cores with special topologies were proposed, designed and analyzed. Most of

these machines were developed for the high performance drive systems, e.g. the axial flux fractional slot concentrated winding machine for the electric vehicle application, the radial flux machine, the 3D transverse flux switched reluctance machine for electric vehicle system, and PM transverse flux machine for light electric vehicle system[8-12].

After having deeply understood the design guidelines for electrical machines with SMC cores, it can be seen that the permanent magnet transverse flux machine (PMTFM) is an ideal machine topology for using SMC materials. Utilizing the global ring windings and 3D magnetic flux path, the PMTFM owns the advantage of high torque capability, as the torque coefficient is proportional to its number of pole pairs, if not saturated [13-15]. The PMTFM can be used for the high torque direct drive applications. However, if it is designed with the silicon steels, the manufacturing process is very complex, and thus the application of this kind of PMTFM has been limited [16-18]. By using SMC materials the manufacturing problem for the PMTFM can be solved. Recently, researchers show great interests in developing and improving the performance of new PMTFM with SMC cores, which includes the design optimization, torque ripple reduction, and manufacturing [19-23].

In [24], a new PMTFM was proposed, in which the PMs are installed on the stator side and thus the flux switching operation principle is used. As the PMs are installed between the stator teeth, large mass PMs can be used on the stator side and thus good flux concentrating effect can be formed. In comparison to the rotor PM TFM, this new kind of machine is named as the stator PM TFM, which can have good torque capability with only use of ferrite magnets. In this paper, a comparative work is conducted on the comparison of rotor PM TFM and stator PM TFM. The operations principle, design methods, magnetic parameters and performance will be studied. The 3D finite element method (FEM) is used for the parameter calculation and it is verified by experiment results.
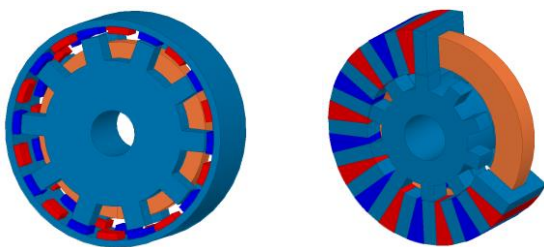
Topology of Rotor PM TFM and Stator PM TFM

Fig. 1(a) shows the finite element model of one phase rotor PM TFM with SMC core. As shown, the motor is designed with the outer rotor configuration, the PMs are surface mounted on the rotor inner surface and the PMs are magnetized along the radial direction. To form three phase symmetrical distribution, the adjacent single phase stator cores are stacked with 120 electrical degrees shifts with each other. Each single phase stator core is composed of two single disks and a global winding in between.

Fig. 1(b) illustrates the main topology of one phase stator PM TFM; similar to the rotor PM TFM, the whole machine is composed of three phases where the adjacent phases have to be shifted with 120 electric degrees with each other. As shown, both the PMs and coils are located on the stator and there is no winding or PM on the rotor. The arrangement of PMs and stator cores can be concluded as that the stator cores and PMs are arranged alternatively and formed with a disk shape, and the adjacent PMs are magnetized along the opposite directions (all the PMs are magnetized along the circumferential direction). The topology of stator PM TFM is quite similar to that of the single phase flux switching permanent magnet machine. However, with the benefits of 3D magnetic isotropy of SMC material, the stator PM TFM is more sophisticated and simple.
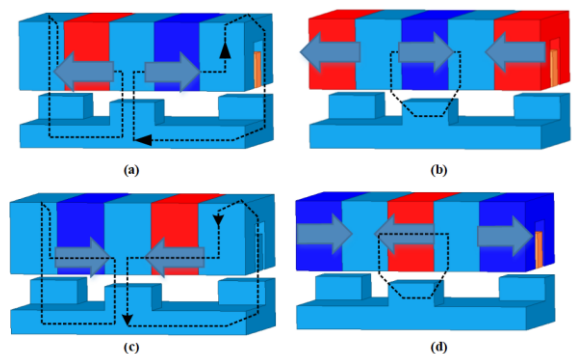

Fig. 2. Main flux path of the stator PM TFM: (a) PM flux (positive maximum), (b) PM flux (zero), (c) PM flux (negative maximum) and (d) PM flux (zero)
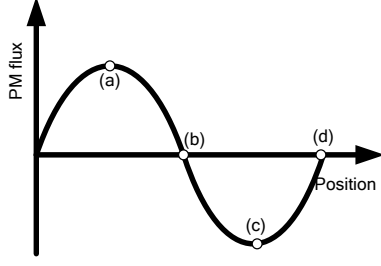
Fig. 3. PM flux linkage of the stator PM TFM against the rotor position.

The operational principle of stator PM TFM can be referenced as that of traditional single phase flux switching permanent magnet machines, but the flux path loop of the new machine is very complex, which can be seen in Fig. 2. As shown in Fig. 2(a), at this position the PM flux will flow along the clockwise direction and the PM flux crossing the winding can reach the positive maximum. When the rotor moves to the right direction and reach the position as shown in Fig. 2(b), the PM flux linkage crossing the winding will be zero. The PM flux linking the winding with the rotor position can be found in Fig. 3.

Power Equation and Qualitative Analysis

To work out the power of electrical machine, the deduction of power equation is a very useful way. It is determined by main dimensions and coefficients, and it can be used to assist researchers to find an optimal design.

Depending on the method to deduce the power equation [7], the electromagnetic torque equation of rotor PM TFM can be obtained as,

$$T_1 = \frac{m_1}{2} P_{r1} k_{l1} K_{sp1} K_{sf1} B_{g1} \pi R_{so1} L_{st1} (L_{l1} - 2L_{st1})(R_{so1} - R_{si1} - h_{sy1}) J_{m1}$$
(1)

$$T_1 / V_1 \propto \sqrt[3]{V_1 \lambda_1^2} \quad (2)$$

where m_1 is the number of phases, P_{r1} the number of pole pairs, k_{l1} the flux leakage coefficient, K_{sp1} the ratio of stator tooth circumference width to the pole pitch, K_{sf1} the slot fill factor, B_{g1} the air gap flux density, R_{so1} the stator outer radius, L_{st1} the stator tooth axial width, L_{l1} the stator core axial length (single phase), R_{si1} the stator inner radius, h_{sy1} the stator yoke thickness, J_{m1} the current density, V_1 the motor volume, and λ_1 the ratio of axial length to outer radius.

By analyzing this torque equation, it can be found that the torque is proportional to the number of pole pairs, and the maximum torque can be obtained when L_{st1} equals a quarter of L_{l1} and at the same time the sum of R_{si1} and h_{sy1} equals the half of R_{so1}. In addition, the torque density is proportional to the volume and λ_1. In the prototype machine, the dimensions of L_{st1}, L_{l1}, R_{si1}, h_{sy1} and R_{so1} are designed to roughly match the above analysis. To obtain the rated frequency of 300 Hz at the rated speed of 1800 rpm, the number of pole pairs is designed as 10.

The torque density of stator PM TFM can be concluded as,

$$\xi_T = \frac{T_2}{m_2 \pi R_{so2}^2 L_{a2}}$$
$$= \frac{\eta P_{r2} B_{g2} K_{s2} K_{d2} K_{sf2} R_{si2}(R_{so2} - R_{si2} - H_{sy2})(L_{a2} - 2W_{st2})W_{st2}J_{m2}}{2R_{so2}^2 L_{a2}}$$
(3)

where T_2, m_2, R_{so2}, L_{a2}, η, P_{r2}, B_{g2}, K_{s2}, K_{d2}, K_{sf2}, R_{si2}, H_{sy2}, W_{st2}, J_{m2} are the output torque, number of phases, stator outer radius, stator axial length, efficiency, number of poles, air gap flux density, ratio of stator tooth length to stator axial length, flux leakage factor, slot fill factor, stator core inner radius, stator yoke thickness, stator tooth width, and current density, respectively. Based on this equation, it can be found that the torque density can be optimized to the maximum value when the W_{st2} equals $0.25L_{a2}$, R_{si2} equals $0.5(R_{so2}-H_{sy2})$, and H_{sy2} should be as minimum as possible. Then the relationship of these parameters and its output torque can be simplified as,

$$(R_{so2} - H_{sy2})^2 L_{a2}^2 = \frac{T_2}{\frac{\eta m_2 P_{r2} B_{g2} \pi K_{s2} K_{d2} K_{sf2} J_{m2}}{64}} \quad (4)$$

Comparing the optimal design of rotor PM TFM and stator PM TFM, it can be seen that the optimized split ratio and the ratio of stator width in the axial direction to the stator slot width in the axial direction are the same. Based on above equations, the main dimension of both rotor PM TFM and stator PM TFM can be obtained, as tabulated in Table 1. Stator PM TFM1 is with ferrite magnet and has the same outer dimension as that of rotor PM TFM. Stator PM TFM2 is with the NdFeB and has the same outer

3

dimension with that of rotor PM TFM. Stator PM TFM3 is with NdFeB and has the same output ability as that of rotor PM TFM.
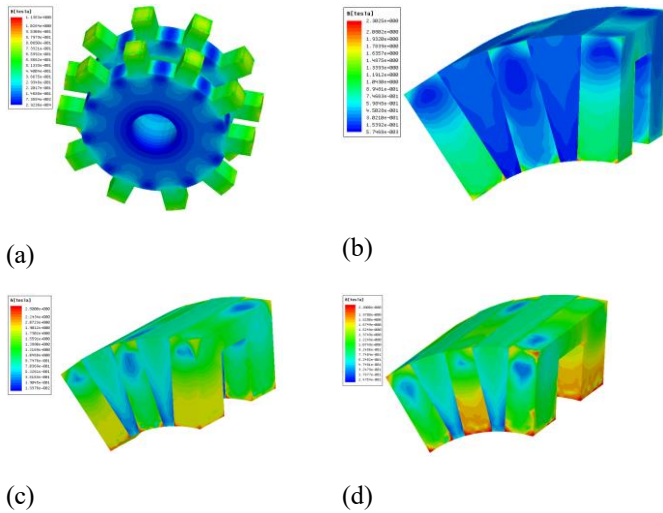
Tab I here

(a)　　　　　　　　　(b)

(c)　　　　　　　　　(d)

Fig. 4. No load flux density distribution: (a) Rotor PM TFM, (b) Stator PM TFM1, (c) Stator PM TFM2, and (d) Stator PM TFM3

Magnetic Field and Parameter Analysis

The no load flux density distributed in the rotor PM TFM and stator PM TFM are shown in Fig. 4, based on 3D FEM. It can be found that the flux density in the stator tooth tips of the rotor PM TFM is 0.7 T, while that of stator PM TFM can reach 1.1 T with only low energy ferrite magnet is used. When NdFeB is used the flux density in the stator tooth tips of the stator PM TFM can even reach 2.0 T, which is close to the magnetic saturation of the SMC material, due to the good flux concentrating effect of the stator PM TFM.

The air gap flux density in the radial direction is illustrated in Fig. 5. It can be seen that the maximum air gap flux density of the rotor PM TFM is about 0.78 T and that of stator PM TFM1, TFM2 and TFM3 is 0.74 T, 1.67 T and 1.59 T respectively. Considering that the average relative permeability of the SOMALOY 500^{TM} is only 200 and the residual flux density of Y35 is only 0.4 T, the magnetic load of the rotor PM TFM1 is very high.

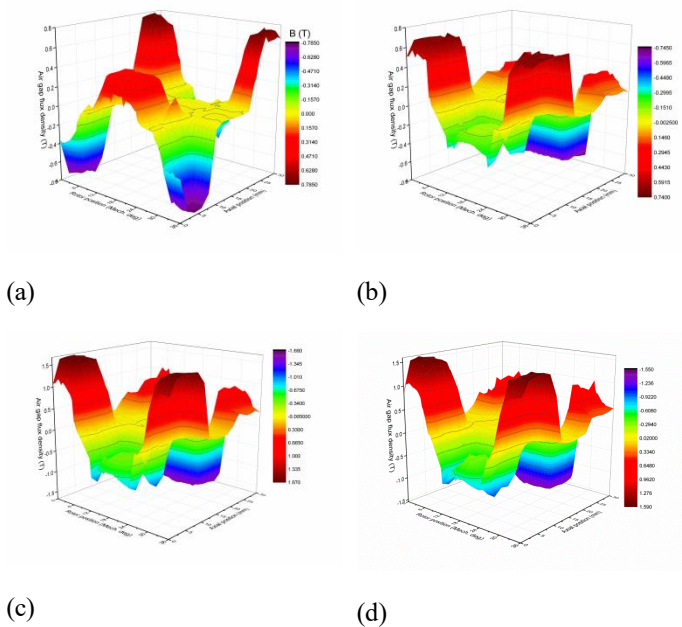
(a)　　　　　　　　　(b)

(c)　　　　　　　　　(d)

Fig. 5. Air gap flux density distribution: (a) Rotor PM TFM, (b) Stator PM TFM1, (c) Stator PM TFM2, and (d) Stator PM TFM3
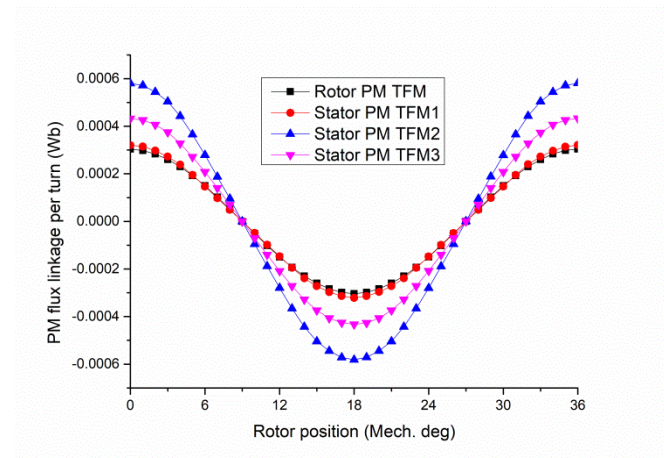
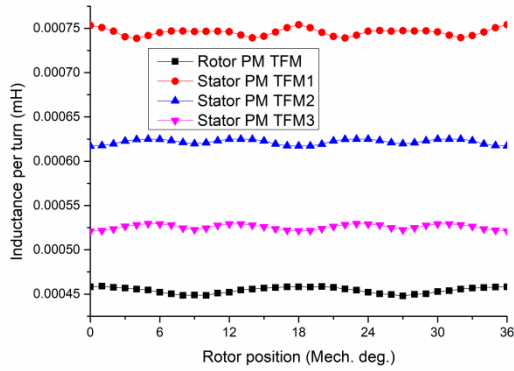Fig. 6. PM flux linkage of the rotor PM TFM and stator PM TFM.

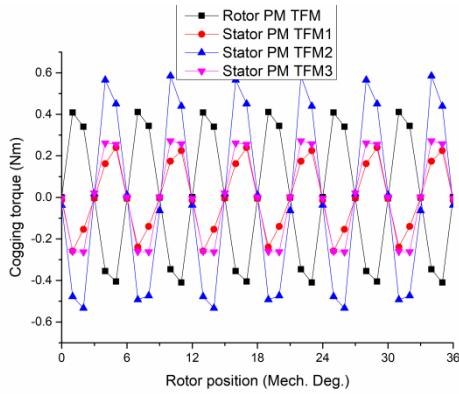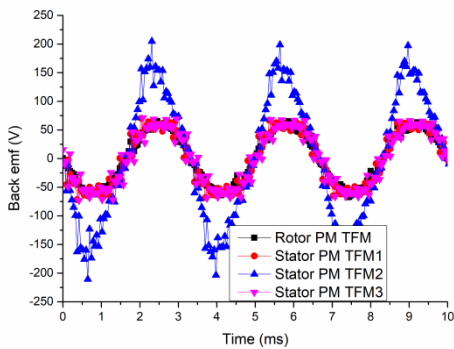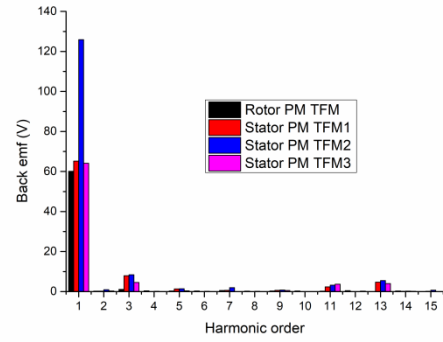Fig. 7. Inductance of the rotor PM TFM and stator PM TFM.

Fig. 8. Cogging torque of the rotor PM TFM and stator PM TFM.

(a)

(b)

Fig. 9. Back EMF of the rotor PM TFM and stator PM TFM, (a) waveforms, and (b) harmonics.

For the permanent magnet machine analysis, the PM flux linkage, inductance and cogging torque are very important. The PM flux linkage, inductance, cogging torque and back EMF of rotor PM TFM, stator PM TFM1, stator PM TFM2 and stator PM TFM3 are shown in Fig. 6 to Fig. 9.

As shown, the PM flux linkage of stator PM TFM2 is the highest, which is resulted by the good flux concentrating structure, high energy PM material and large dimensions with the same number of pole pairs. The PM flux linkage of stator PM TFM3 is the second highest, and the stator PM TFM1 has the same flux linkage as that of rotor PM TFM.

For the inductance comparison, as shown in Fig. 7, the average inductance of stator PM TFM1 is higher than that of other TFMs, which is calculated by using the frozen permeability technology. The main reason is that the adopted ferrite magnet material has caused the stator PM TFM1 to have low magnetic load, and thus the main magnetic resistance of the TFM is lower than the other TFMs. The average inductance of rotor PM TFM is the lowest, and the main reason is that the leakage flux path is short. It can be found that the variation of inductance with the rotor angles for all four TFMs is very small, thus the difference between the d-axis inductance and q-axis inductance is also very small, and the reluctance torque component in this machine can be ignored and only the PM torque contributes to the main torque.

The cogging torque is resulted by the interaction between the PMs on the rotor or stator and the stator slots or rotor slots, which can bring the machine with vibration and noise. In a complete period of the

5

operation, the average of the cogging torque is zero, but it produces the torque ripple. For the TFMs, the cogging torque is obtained by the addition of the cogging torque from the single phase with determined angle shifts. As shown in Fig. 8, the peak value of the cogging torque in the stator PM TFM2 is the highest. The cogging torque of rotor PM TFM is the second highest. As all these TFMs are designed with same number of poles, and the period for the cogging torque is the same.

Fig. 9 shows the back EMF comparison among these TFMs. As can be seen, the stator PM TFM2 has the highest magnitude of back EMF, and the other TFMs have the similar magnitude of back EMF. All these TFMs have the sinusoidal back emf waveforms. For the harmonic analysis, all the TFMs has similar high order harmonics, e.g. 3rd, 11th and 13rd harmonics are the main harmonics.

Performance Calculation

For evaluation of the performance of PM machines, the torque ability, core loss characteristic, power factor, efficiency and cost are the key factors. Considering that these TFMs have very low saliency ratio, the control method with zero d-axis current is used for the torque calculation, and only the PM torque are considered.
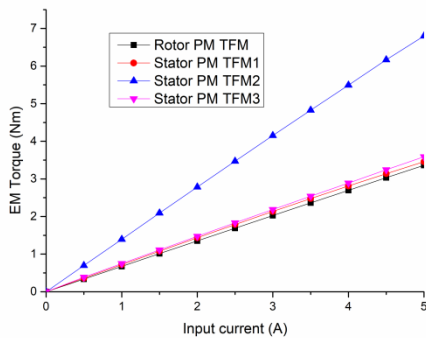
(a)
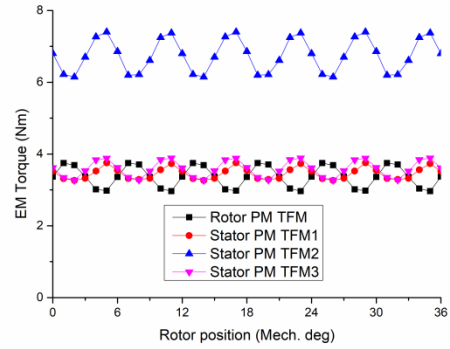
(b)

Fig. 10. Torque ability of the rotor PM TFM and stator PM TFM versus (a) input current, and (b) rotor position.
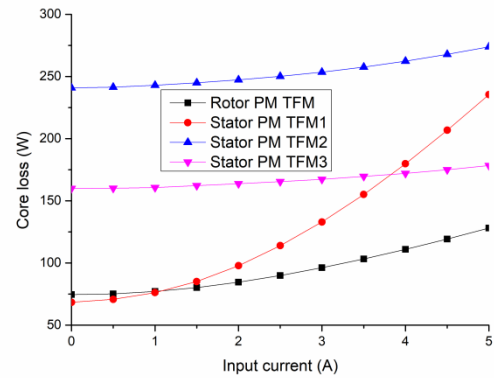

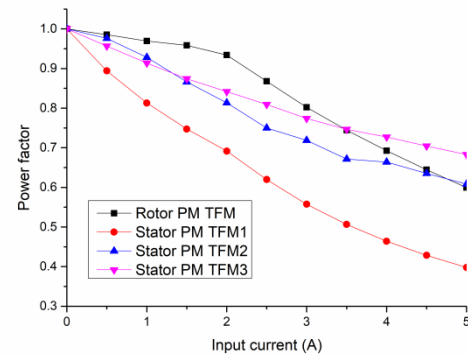Fig. 11. Core loss of the rotor PM TFM and stator PM TFM.

Fig. 12. Power factor of the rotor PM TFM and stator PM TFM.

The relationship between the electromagnetic torque and input current is shown in Fig. 10. It can be found that the torque ability of the stator PM TFM2 is the highest while the other TFMs have quite similar torque ability. As shown in Fig. 10(b),

the torque ripple of stator PM TFM2 is the highest at the rated condition while the others have the similar torque ripple. It can be seen that in these TFMs, the cogging torque contributes the main torque ripple if comparing Fig. 10(b) with the Fig. 8. In this work these TFMs are designed for the small application and no additional cooling techniques are used, thus the current density is designed not too high, lower than 6 A/mm². It can be seen that with this kind of current density, the torque has the linear characteristic with the current.

Core loss is another important factor in the electrical machine analysis. For the PM TFM, the core loss is determined by the operation frequency and magnetic flux density in the stator core. To calculate the core loss, the multi frequency core loss properties of the SMC material is used in the transient module in the MAXWELL 3D package. The core loss of these TFMs is shown in Fig. 11. It can be seen that the core loss of stator PM TFM1 increases quickly with the increase of input current, due to the magnetic flux distributed in the machine at the no load state is relatively low. When the input current increases, magnetic flux density increases more quickly than the TFMs with NdFeB. As the stator PM TFM2 is designed with higher power rating, the core loss of stator PM TFM2 is the highest .

To drive the PM TFM, a three phase power electronic device is required. Power factor is defined by output power divide input voltage ampere, and the lower power factor means that higher rating invert bridge is needed in the drive system, then the whole system cost will be increased. In the PM TFM, as the inductance is much higher than the winding resistance, to simplify the power factor definition, the effect of resistance can be neglected, and thus the power factor can then be defined as,

$$PF = 1 \Big/ \sqrt{1 + L_s I_q / \Psi_{pm}} \quad (5)$$

where L_s is the inductance, I_q the q-axis current and Ψ_{pm} the PM flux linkage. It is obvious that increasing the number of pole pairs will reduce the power factor, as the PM flux will be reduced and leakage inductance will be increased. Fig. 12 shows the power factor of rotor PM TFM and stator PM TFM with different input currents at the rated speed. It can be seen that the stator PM TFM1 has the lowest power factor and the power factor of all PM

TFMs decreases with the increase of input current. For the TFM with NdFeB, it can be seen that with the current of not too high value, the rotor PM TFM has high power factor. However, when the input current is increased to a determined value, the power factor of stator PM TFM will be higher than that of rotor PM TFM. Therefore, the stator PM TFM has higher potential for the high power machine design and high load operation.
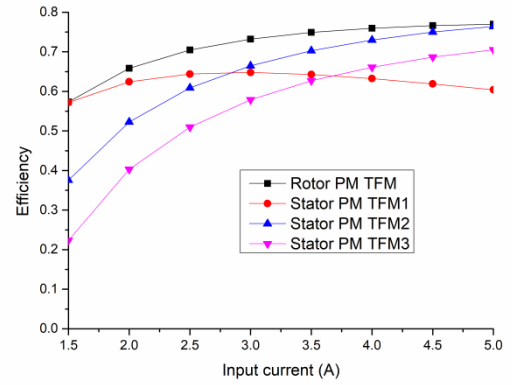

Fig. 13. Efficiency of the rotor PM TFM and stator PM TFM.

The output power and efficiency are the specified parameters of the PM TFM. The output power and efficiency can be calculated by following equations,

$$P_{out} = P_{em} - P_{Core} - P_{mech}$$

$$\eta = P_{out} \big/ (P_{em} + P_{cu})$$

where P_{em} is the electromagnetic power, P_{core} the core loss, P_{mech} the mechanical loss, and P_{cu} the copper loss.

The electromagnetic power is calculated by multiplying the electromagnetic torque obtained from FEM and designed rotor speed. The core loss can be obtained from the core loss analysis. The mechanical loss contains the friction loss and windage loss, and in this paper it is estimated as 1.5% of output power. The copper loss is obtained by $3I^2R$. Fig. 13 shows the efficiency comparison of the rotor PM TFM and stator PM TFM. It can be seen that the efficiency of rotor PM TFM is high when the input current is not too high. However, with the increase

of input current, the efficiency of stator PM TFM2 will be the highest one. If comparing the effect of NdFeB and ferrite magnet excitation, it can be seen that the stator PM TFM with ferrite magnet has the lowest efficiency.
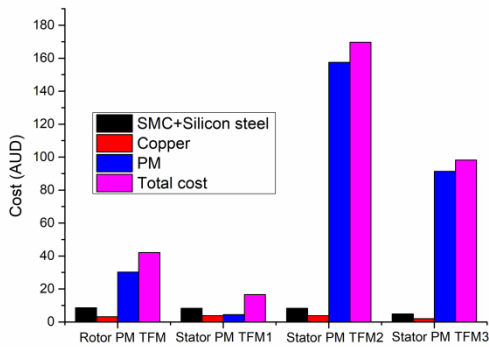

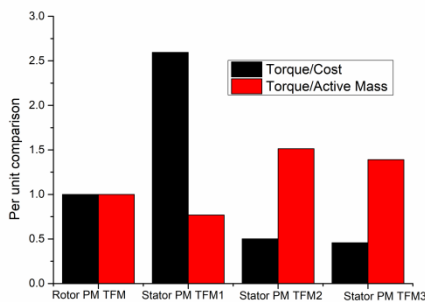Fig. 14. Cost of the rotor PM TFM and stator PM TFM.

Fig. 15. Overall comparison of the rotor PM TFM and stator PM TFM.

Fig. 14 shows the cost comparison among these TFMs, and it can be seen that the NdFeB plays the main role in the material cost. For the stator PM TFM1 with ferrite magnet, the total cost is much lower than the others. Fig. 15 shows the per unit overall comparison. It can be seen that the torque/cost of the stator TFM1 is the highest one and it is about 2.5 times higher than the rotor PM TFM, while for the torque/active mass comparison, as the stator PM TFM1 has more compact structure with more copper, its torque/active mass is the lowest one, even it can output the same torque ability as that of rotor PM TFM.
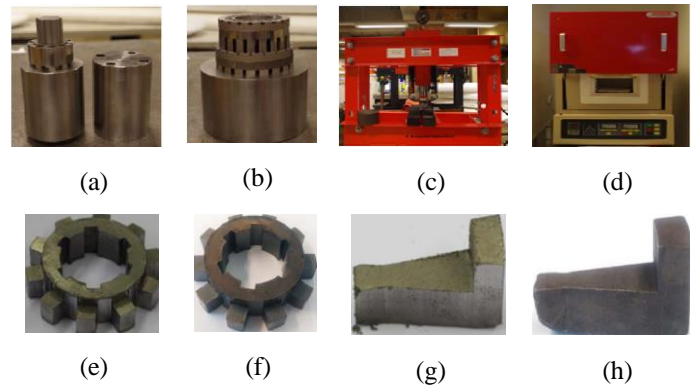

Fig. 16. Die tools, facilities and SMC cores for the stator PM TFM, (a) die tools for compaction of rotor core, (b) die tools for compaction of stator cores, (c) compact machine, (d) furnace, (e) rotor core before heat treatment, (f) rotor core after heat treatment, (g) stator core before heat treatment, and (h) stator core after heat treatment
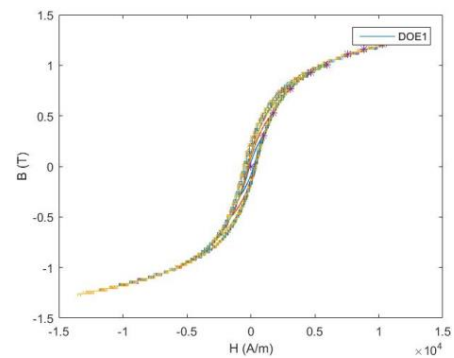

Fig. 17. Magnetic hysteresis loop of the rotor core.

Manufacturing of SMC cores

In the university laboratory, the manufacturing of SMC cores for determined electric machines can use three methods, wire cutting, mechanical machining and manual die compaction. By using the former two methods, the electromagnetic properties of the SMC core can be deteriorated, so the manual die compaction method is recommended for the SMC core fabrication. Fig. 16 shows the tools which are necessary for the manual die compaction and heat treatment process of the SMC cores for the stator PM TFM.

Fig. 17 shows the measured magnetic hysteresis loop of the SMC rotor core for stator PM TFM. When the stator cores and rotor cores are obtained, the assembly process of the stator PM TFM can be started. To make the machine with good mechanical strength, the global winding and the stator cores will

be formed as a whole part by using the plastic injection molding technology and the special winding with the cross area of rectangle structure will be used to improve the slot fill factor.
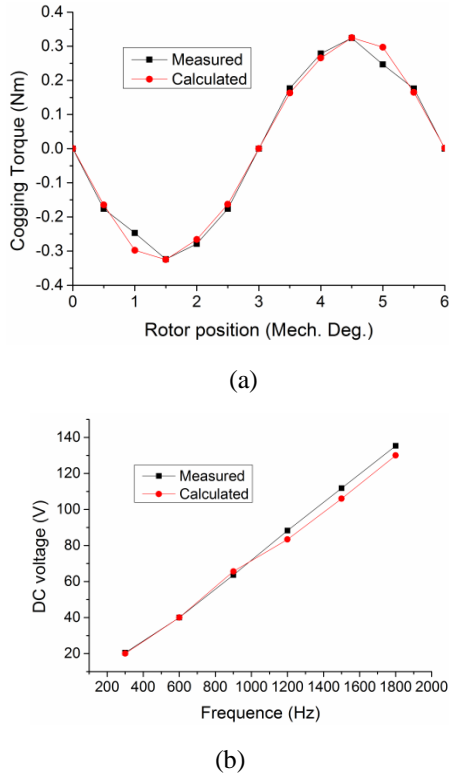

(a)

(b)

Fig. 18. Comparison of the measured and calculated results of rotor PM TFM: (a) cogging torque, and (b) DC voltage

Experimental Validation

To verify the 3D FEM results, the experiment results of the rotor PM TFM are presented. Fig. 18 compares the calculated and measured cogging torque and DC voltage values. It can be found that the calculated results match well with the measured ones. The measured cogging torque has a small variation at the positions of 1 deg. and 5 deg., which is different from the calculated ones. It may be resulted by the leakage flux distraction from the adjacent phase. The calculated and measured inductances are 6.75 and 6.53 mH, respectively. The calculated resistance of the winding is 0.31 Ω and the measured one is 0.305 Ω. For the rated operation situation, the calculated core loss is 128 W, and the measured one is 112 W. For the no load situation, the calculated core loss is 72 W and the measured one is 61 W. The calculated efficiency of the PMTFM at

the rated state is 81%, while the measured one is 79.5%. The error may be resulted by the rotor yoke eddy current loss, and the magnet losses.

Conclusion

In this paper, the comparative study work between the rotor PM TFM and stator PM TFM is conducted. For the deep comparison, four TFMs are designed. The first is a rotor PM TFM with NdFeB magnet, the second is a stator PM TFM1 with ferrite magnet, and the third and forth are stator PM TFM2 and TFM3 with NdFeB. Rotor PM TFM, and stator PM TFM1, and TFM2 have the same outer dimensions, and the stator PM TFM3 has the same output power ability as that of rotor PMTFM. The stator PM TFM is based on the flux switching operation principle and thus good flux concentrating structure can be formed. Another advantage for stator PM TFM is that all the windings and PMs are installed on the stator side, thus the mechanical robust characteristic can be improved. Based on the deduced power equation, it can be seen that both the stator PM TFM and rotor PM TFM can be designed with the same split ratio and ratio of stator slot to stator width to achieve the highest torque ability.

With the utilization of ferrite magnet, though the stator PM TFM1 has good flux concentrating structure and it can have the same torque ability as the rotor PM TFM, it has lower power factor and efficiency. However, the material cost of this machine is very low, thus it can be used for the home appliance, where the cost needs to be considered at the first order. For the stator PM TFM2 and TFM2 with NdFeB, they show very good performance of torque ability, power factor and efficiency. Especially the input current can be high, thus the stator PM TFM with NdFeB is more suitable for the high performance drive application.

Reference

[1] A. Krings, A. Boglietti, A. Cavagnino, and S. Sprague, "Soft magnetic material status and trends in electric machines," IEEE Trans. Ind. Electron., vol. 64, no. 3, pp. 2405-2414, Mar. 2017

[2] A. Schoppa and P. Delarbre, "Soft magnetic powder composites and potential applications in modern electric machines and devices," IEEE

9

Trans. Magn., vol. 50, no. 4, article #: 2004304, 2014.

[3] J. Potgieter, F. Fernandez, A. Fraser, and M. Mcculloch, "Effects observed in the characterization of soft magnetic composite for high frequency, high flux density applications," IEEE Trans. Ind. Electron., vol. 64, no. 3, pp. 2486-2493, Mar. 2017

[4] J.G. Zhu, Y.G. Guo, Z.W. Lin, Y.J. Li, Y.K. Huang, "Development of PM transverse flux motors with soft magnetic composite cores," IEEE Trans. Magn., vol. 47, no. 10, pp. 4376-4383, Sep. 2011.

[5] A.G. Jack, "Permanent magnet machines with powdered iron cores and prepressed windings," IEEE Trans. Ind. Appl., vol. 48, no. 11, pp. 1077-1084, Jul./Aug. 2000

[6] Y. G. Guo, J. G. Zhu, P. A. Watterson, and W. Wu, "Development of a PM transverse flux motor with soft magnetic composite core," IEEE Trans. Energy Convers., vol. 21, pp. 426-434, 2006.

[7] C. C. Liu, G. Lei, T.S. Wang, Y.G. Guo, Y.H. Wang and J.G. Zhu, "Comparative study of small electrical machines with soft magnetic composite cores," IEEE Trans. Ind. Electron., vol. 64, no. 2, pp. 1049-1060, Feb. 2017

[8] B. Zhang, T. Seidler, R. Dierken and M. Doppelbauer, "Development of a Yokeless and Segmented Armature Axial Flux Machine", IEEE Trans. Ind. Electron., vol. 63, no. 4, pp. 2062-2071, April 2016.

[9] J. Doering, G. Steinborn and W. Hodman, "Torque, power, losses, and heat calculation of a transverse flux reluctance machine with soft magnetic composite materials and disk shaped rotor," IEEE Trans. Ind. Appl., vol. 51, no. 2, pp. 1494-1504, Mar./Apr. 2015

[10] J. Washington, J. Atkinson, et al., "Three phase modulated pole machine topologies utilizing mutual flux paths," IEEE Trans. Energy Conve., vol. 27, no. 2 pp: 507-515, 2012

[11] Y.S. Kwon, and W. J. Kim, "Electromagnetic analysis and steady-state performance of double sided flat linear motor using soft magnetic composite," IEEE Trans. Ind. Electron., vol. 64, no. 3, pp. 2178-2187, Mar. 2017

[12] T. Ishikawa, K. Takahashi, H.Q. Viet, M. Matsunami, and N. Kurita, "Analysis of novel brushless DC motors made of soft magnetic composite core," IEEE Trans. Magn., vol. 48, no. 11, pp. 971-974, Feb. 2012.

[13] J.R. Anglada, S. M. Sharkh, "An insight into torque production and power factor in transverse flux machines," IEEE Trans. Ind. Appl., vol. 53, no. 3, pp. 1971-1977, May./Jun. 2015

[14] T. Husain, I. Hasan, Y. Sozer, I. Husain, and E. Uuljadi, "Design considerations of a transvers flux machine for direct dirve wind turbine applications," IEEE Trans. Ind. Appl., vol. 54, no. 4, pp. 3604-3615, July/Aug. 2018

[15] A. Ahmed, and I. Husain, "Power factor improment of a transverse flux machine with high torque density," IEEE Trans. Ind. Appl., vol. 54, no. 5, pp. 4297-4305, Sept./Oct. 2018

[16] Y. G. Guo, J. G. Zhu, and D. G. Dorrell, "Design and analysis of a claw pole permanent magnet motor with molded soft magnetic composite core," IEEE Trans. Magn., vol. 45, pp. 4582-4585, 2009.

[17] X. Li, W. Xu, C.Y. Ye, and I. Boldea, "Comparative study of transverse flux permanent magnetic linear oscillatory machines for compressor," IEEE Trans. Ind. Electron., vol. 65, no. 9, pp. 7437-7446, Sept. 2018

[18] M.Q. Wang, P. Zheng, C.D. Tong, Q.B. Zhao, and G.Y. Qiao, "Research on a transverse flux brushelss double rotor machine for hybrid electric vehicles," IEEE Trans. Ind. Electron., vol. 66, no. 2, pp. 1032-1043, Feb. 2019

[19] M. Zhao, Y. Wei, H.Y. Wang, M.M. Hu, F.J. Han and etc., "Development and analysis of novel flux switching transverse flux permanent magnet linear machine," IEEE Trans. Ind. Electron., vol. 66, no. 6, pp. 4923-4933, FJune 2019

[20] X Zhao, and S.X. Niu., "Development of a novel transverse flux tubular linear machine with parallel and complemerntary PM magnetic circuit for precision industrial processing," IEEE Trans. Ind. Electron., vol. 66, no. 6, pp. 4945-4955, FJune 2019

[21] T. Husain, I. Hasan, Y. Sozer, I. Husain, and E. Uuljadi, "Cogging torque minzation in transverse flux machines," IEEE Trans. Ind. Appl., vol. 55, no. 1, pp. 385-397, Jan./Feb. 2019.

[22] B. Ma, G. Lei, J.G. Zhu, Y.G. Guo, and C.C. Liu, "Application-oriented robust design optimization for batch production of permanent magnet motors," IEEE Trans. Ind. Electron., vol. 65, no. 2, pp. 1728-1739, Feb. 2018

[23] G. Lei, T. S. Wang, Y. G. Guo, J. G. Zhu, and S. H. Wang, "System level design optimization methods for electrical drive systems: deterministic approach," IEEE Trans. Ind. Electron., vol. 61, no. 12, pp. 6591-6602, Dec. 2014.

[24] C. C. Liu, J. G. Zhu, Y. H. Wang, et al., "Development of a new low cost 3-D flux transverse flux FSPMM with soft magnetic composite cores and ferrite magnets," IEEE Trans. Magn., vol. 51, no. 11, article# 8110904, 2015

Table 1 Main Dimensions and Parameters of Rotor PM TFM and Stator PM TFM

Parameter	Rotor PM TFM	Stator PM TFM1	Stator PM TFM2	Stator PM TFM3
Stator outer radius	40 mm	47 mm	47 mm	36 mm
Stator inner radius	9.5 mm	28 mm	28 mm	22 mm
Rotor outer radius	47 mm	27.5 mm	27.5 mm	21.5 mm
Axial length	3*31mm	3*31mm	3*31mm	3*31mm
Stator tooth width	9 mm	10 mm	10 mm	10 mm
Stator yoke height	10.5 mm	5 mm	5 mm	4 mm
Coil turns	125	125	125	85
PM material	NdFeB	Ferrite	NdFeB	NdFeB